Blood Clots Are Rapidly Assembled Hemodynamic Sensors
Flow Arrest Triggers Intraluminal Thrombus Contraction

Ryan W. Muthard, Scott L. Diamond

Objective—Blood clots form under flow during intravascular thrombosis or vessel leakage. Prevailing hemodynamics influence thrombus structure and may regulate contraction processes. A microfluidic device capable of flowing human blood over a side channel plugged with collagen (±tissue factor) was used to measure thrombus permeability (κ) and contraction at controlled transthrombus pressure drops.

Methods and Results—The collagen ($\kappa_{collagen}=1.98\times10^{-11}$ cm^2) supported formation of a 20-μm thick platelet layer, which unexpectedly underwent massive platelet retraction on flow arrest. This contraction resulted in a 5.34-fold increase in permeability because of collagen restructuring. Without stopping flow, platelet deposits (no fibrin) had a permeability of $\kappa_{platelet}=5.45\times10^{-14}$ cm^2 and platelet-fibrin thrombi had $\kappa_{thrombus}=2.71\times10^{-14}$ cm^2 for ΔP=20.7 to 23.4 mm Hg, the first ever measurements for clots formed under arterial flow (1130 s^{-1} wall shear rate). Platelet sensing of flow cessation triggered a 4.6- to 6.5-fold (n=3, $P<0.05$) increase in contraction rate, which was also observed in a rigid, impermeable parallel-plate microfluidic device. This triggered contraction was blocked by the myosin IIA inhibitor blebbistatin and by inhibitors of thromboxane A2 (TXA_2) and ADP signaling. In addition, flow arrest triggered platelet intracellular calcium mobilization, which was blocked by TXA_2/ADP inhibitors. As clots become occlusive or blood pools following vessel leakage, the flow diminishes, consequently allowing full platelet retraction.

Conclusion—Flow dilution of ADP and thromboxane regulates platelet contractility with prevailing hemodynamics, a newly defined flow-sensing mechanism to regulate clot function. **(*Arterioscler Thromb Vasc Biol*. 2012;32:2938-2945.)**

Key Words: ADP ■ coagulation ■ hemodynamics ■ thrombosis ■ thromboxane

During thrombosis or hemostasis under flow conditions, platelets rapidly deposit at the site of vascular injury. The vessel wall and subendothelium quickly become connected mechanically to the developing thrombus.[1] During vessel wound closure, this interwoven assembly prevents further blood loss by platelet-mediated clot contraction and stiffening.[2] Platelets generate contractile forces to allow clots to match the stiffness of the endothelium.[3] Interactions between myosin II and actin filaments govern this contraction and are regulated by the activation of myosin light chain kinase through calcium/calmodulin and Rho kinase signaling.[4,5] During contraction, force transmission ultimately occurs via talin and $\alpha_{IIb}\beta_3$, which binds platelets via fibrinogen and fibrin.[6,7] Following clot retraction, the tight seal that is formed around the injured tissue significantly reduces clot permeability, consequently limiting the leakage of cells and plasma. Also, the permeability of occlusive clots is critical to thrombolytic therapy for acute myocardial infarction because permeation dictates penetration of plasminogen activators.[8] The effects of local hemodynamics on clot contraction and permeability are poorly understood, yet highly relevant to thrombus growth, stability, or susceptibility to embolism, fibrinolysis, or bleeding.

Prior studies of clot permeability have used whole blood clots that do not achieve the 50- to 100-fold increase in platelet concentration on a surface that occurs under flow conditions.[9,10] Although clot contraction has been studied for decades using clots formed in test tubes, there exists a large gap in the fundamental understanding of mechanisms that initiate and control the response under hemodynamic conditions. In terms of force-loading of thrombotic structures, platelets respond with larger stall forces when exposed to stiffer fibrinogen-coated atomic force microscopy cantilevers.[3] Studies of whole clot contraction forces may not necessarily predict clot contraction dynamics under flow conditions.

We measured, for the first time, clot contractility and permeability under hemodynamic conditions. The presence of tissue factor (TF) caused a significant decrease in thrombus permeability. Unexpectedly, flow arrest caused enhancement of permeability for platelet deposits because of a triggered clot contraction and consequent collagen restructuring. To further examine platelet contraction after flow cessation, a rigid

Received on: August 15, 2012; final version accepted on: October 3, 2012.

From the Institute for Medicine and Engineering, Department of Chemical and Biomolecular Engineering, Vagelos Research Laboratory, University of Pennsylvania, Philadelphia, PA.

The online-only Data Supplement is available with this article at http://atvb.ahajournals.org/lookup/suppl/doi:10.1161/ATVBAHA.112.300312/-/DC1.

Correspondence to Scott L. Diamond, University of Pennsylvania, 394 Towne Bldg, 220 S 33rd St, Philadelphia, PA 19104. E-mail sld@seas.upenn.edu

wall flow device was used. Platelet deposits were developed and antagonized using blebbistatin, a myosin II inhibitor, and ADP/TXA_2 receptor antagonists. Flow arrest caused an intracellular increase in Ca^{2+} that preceded contraction and was dependent on the autocrine signaling of ADP and TXA_2. These studies provide new insight into the ability of platelets to sense local hemodynamic flow based on the convective-diffusive transport of autocrine signaling molecules.

Materials and Methods

Reagents

The following reagents and instrumentation were obtained and stored according to manufacturers' instructions: polydimethylsiloxane (Ellsworth Adhesives); sigmacote, streptavidin, sulforhodamine 101 acid chloride (Texas Red), fluorescein isothiocyanate, and 2-methylthioadenosine 5'-monophosphate triethylammonium salt hydrate (2-MeSAMP; Sigma-Aldrich); human type-1 monomeric collagen (VitroCol, 3 mg/mL; Advanced Biomatrix); equine tendon-derived type-1 fibrillar collagen (Chrono-log); biotinylated goat anticollagen type I polyclonal antibody (Abcam); 0.05 µm Fluoresbrite microspheres (Polysciences Inc); Fluo-4-no wash (Life Technologies); blebbistatin (EMD Millipore); [1S-[1 alpha,2 beta (5Z),3 beta,4 alpha]-7-[3-[[2-[(phenylamino) carbonyl]hydrazino]methyl]-7-oxabicyclo[2.2.1] hept-2-yl]-5-heptenoic acid (SQ 29,548; Cayman Chemical); 2′-Deoxy-N6-methyladenosine 3′,5′-bisphosphate tetrasodium salt (MRS-2179; Tocris Bioscience); antifibrin antibody (gift from the M. Poncz, Children's Hospital of Philadelphia); L-α-phosphatidylserine, L-α-phosphatidylcholine, and biotinylated phosphatidylethanolamine (Avanti Polar Lipids); and analog pressure transducers (Honeywell Sensing and Control).

Blood Collection

All donors were reported as medication-free for the previous 10 days, and blood collection was in accordance with the University of Pennsylvania's Institutional Review Board. Human blood from healthy volunteers was collected into 100 µmol/L Phe-Pro-Arg-chloromethylketone (PPACK, Haematologic Technologies Inc) or 40 µg/mL corn trypsin inhibitor (Haematologic Technologies Inc). PPACK-treated whole blood was also treated with fluorescently conjugated anti-CD41 monoclonal antibody (1 µg/mL; Abd Serotec). Phycoerythrin-conjugated anti-CD61 (0.125 µg/mL; Becton Dickinson Biosciences) and fluorescently conjugated anti-fibrin antibodies (0.5 µg/mL) were added to corn trypsin inhibitor-treated blood as previously described.[11,12]

Permeation Device Design and Manufacture

Polydimethylsiloxane was used to construct microfluidic devices following soft lithography protocols[13] as previously described.[14–16] The primary blood flow channel (250 µm wide×60 µm high) was designed to create flow over a micropost scaffold region as illustrated in Figure 1A. At this micropost scaffold junction, blood could continue along the primary channel or exit through the scaffold channel (50 µm wide×60 µm high) to an outlet port maintained at P3=atmospheric pressure or blocked so that P3 equals the pressure within the blood flow channel. Real-time pressure measurements were collected in LabVIEW (National Instruments) using 0 to 1 psig pressure transducers upstream (P2), downstream (P1), and exiting the scaffold region (P3) as shown in Figure 1. Channel pressure was controlled using 2 constant volume syringe pumps (Harvard Apparatus). A syringe pump located upstream of the collagen scaffold delivered anticoagulated whole blood at an independently controlled initial inlet wall shear rate (1130 s^{-1}), whereas a downstream pump perfused Ca^{2+} buffer (5 mmol/L) at a rate set by a proportionate controller programmed in LabVIEW.

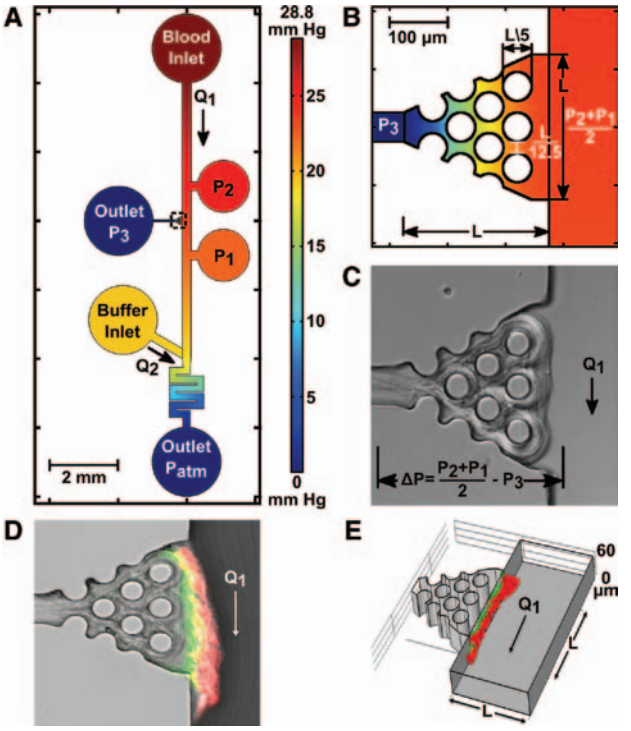

Figure 1. Microfluidic device to independently control blood flow and transthrombus pressure drop. COMSOL was used to determine the pressure throughout the microfluidic device (**A**) including the collagen scaffold region (**B**), where L=250 µm. Human type I polymerized collagen was localized in the scaffold region (**C**). After 10 minutes of corn trypsin inhibitor (CTI)-whole blood flow at 1130 s^{-1}, platelets (red), fibrin (green), and their overlap (yellow) form a thrombus on the collagen (**D**). A confocal image of platelets (red) and fibrin (green) shows the 3D structure of the microfluidic device (**E**).

Microfluidic Device for Thrombus Permeation

Polydimethylsiloxane devices were sealed to Sigmacote-treated glass slides using vacuum-assisted bonding. Type I human monomeric collagen solution was polymerized at 2.4 mg/mL overnight using 8 parts collagen, 1 part 0.09 M NaOH, and 1 part 10x PBS. Before loading the scaffold with collagen, all channels were incubated with 10% BSA for 30 minutes at room temperature. After incubation, well-mixed polymerized collagen solution was pipette on the upstream and downstream pressure ports and localized into the micropost scaffold region by pulling the solution (2.5 µL) through the scaffold exit channel with syringe withdraw for ≈15 seconds. A fixed amount of collagen (≈3.3 ng) was thus deposited on the micropost scaffold. Collagen solution remaining in the channel region (between P2 and P1) was removed by infusion of Ca^{2+} buffer (5 mmol/L) from the blood inlet port before instillation of blood for the experiment. For experiments using collagen with linked TF, biotinylated and TF liposomes (20:79:1, L-α-phosphatidylserine/L-α-phosphatidylcholine/biotinylated phosphatidylethanolamine) were prepared as previously described[15,16] following the method of Smith et al.[17] Polymerized collagen (2.4 mg/mL) was mixed in a 10:1 ratio by volume with biotinylated anticollagen (4 µg/mL) and incubated at room temperature for 5 minutes. Streptavidin (10 µg/mL) at a 1:10 volumetric ratio and TF liposomes at a 1:20 volumetric ratio with collagen were sequentially added and incubated for 5 and 10 minutes, respectively. The fibrillar collagen/TF solution was then perfused through the micropost array region as described for fibrillar collagen.

Permeability Measurements

Whole blood was anticoagulated with PPACK for perfusion over collagen or with corn trypsin inhibitor for perfusion over

collagen/TF. Each whole blood perfusion was conducted at an inlet wall shear rate of 1130 s^{-1} for 10 minutes. The transthrombus pressure drop was immediately set to the controlled value and side view images of the platelet or platelet/fibrin thrombus were taken at the blood contact region of the collagen scaffold. After thrombus development, an injection valve (Idex Health & Science) was manually switched to pulse Ca^{2+} buffer (5 mmol/L) containing Texas Red or fluorescein isothiocyanate dye (≈25 μL) without disruption of the flow. Real-time dye, platelet, and fibrin fluorescent intensities were imaged with an inverted microscope (IX81, Olympus America Inc) using a charge-couple device camera (ORCA-ER, Hamamatsu). Confocal images of platelet/fibrin thrombus were taken in 2-μm sections, under flow, with a disk-scanning unit (IX2, Olympus America). ImageJ software was used to analyze all images and develop 3-dimensional representations of thrombus.

Contraction Measurements

PPACK-treated whole blood with or without the addition of 50 nm fluorescent microspheres (10^{10} beads/mL blood) was perfused through the permeation device at 1130 s^{-1}. Platelet deposits were formed for 10 minutes under a constant transthrombus pressure drop (23.5 mm Hg). Whole blood flow was then switched without interruption to Ca^{2+} buffer (5 mmol/L) flow. After 4.5 minutes of buffer flow, both syringe pumps were stopped and the transthrombus pressure drop immediately approached zero. Platelet deposits were imaged in 15-seconds intervals for 30 minutes.

Thrombus contraction studies were also performed in a parallel channel microfluidic device.[14] Briefly, a microfluidic device was used to print a 250 μm wide strip of diluted fibrillar collagen lengthwise on a Sigmacote-treated glass slide. The patterning device was removed and a second device was positioned with 10 parallel channels (250 μm wide×60 μm high) perpendicular to the collagen. All channels were preincubated with 0.5% BSA. Anticoagulated whole blood (PPACK) was treated with or without an intracellular Ca^{2+} dye. Fluo-4-no wash (2.5 mmol/L probenecid) was loaded into platelets by incubating 1 part dye with 4 parts blood for 45 minutes. Dye treated or untreated blood was then placed in the inlets of 3 channels. A syringe pumped allowed simultaneous perfusion of the 3 channels at an initial wall shear rate of 1160 s^{-1}. After the collagen patches (250×250 μm) were covered with platelets, flow was immediately switched to Ca^{2+} buffer (5 mmol/L, 0.01% dimethyl sulfoxide) in the presence or absence of antagonist (blebbistatin or mixtures of SQ-29,548, MRS-2179, 2-MeSAMP). In some experiments, buffer flow was stopped (30 seconds or 1 minute) and then re-established or completely stopped after 7 minutes of perfusion. Intracellular Ca^{2+} fluorescence and platelet deposit structures were imaged with a 20x objective, in 15-second intervals, for the duration of the experiment.

Finite Element Analysis

COMSOL Multiphysics software was used to numerically solve steady state pressure gradients, blood flow velocities, and permeation velocities over complex geometries (collagen plus thrombus) with constant permeability in the polydimethylsiloxane permeation device. Blood (ρ=1060 kg/m^3, μ=0.003 Pa·s) and buffer (ρ=1000 kg/m^3, μ=0.001 Pa·s) were both modeled using laminar flow for solution of the Navier-Stokes equation (Re=0.49, $Re_{element}$=0.25). The collagen region was modeled using Darcy's law ($\nabla^2 P$=0) with entrance and exit pressures being coupled to the external laminar flow properties and permeability (κ) set to a previously determined value (eg, $\kappa=1\times10^{-15}$ m^2).[18] Flow rates of 13 μL/min for blood and buffer allowed the downstream resistance length to be modified to achieve ΔP=23.5 mm Hg at the collagen scaffold interface.

Collagen, platelet, and platelet/fibrin permeability were each solved in COMSOL for the complex geometries of the collagen scaffold and developed thrombus. Calculating and comparing the permeability of collagen to previously reported values provided experimental validation of the device.[18,19] Experimental pressure and calculated average velocity data were used as input parameters. The square difference between the experimental and computational average velocity across the collagen scaffold were iteratively reduced (<0.001 $\mu m^2/s^2$) by varying the collagen permeability. With the solved collagen permeability, the process was repeated for the platelet or platelet/fibrin geometry on the collagen. The normalized dye concentration in the channel was used as transient input data into the model. Matching the transient pulse concentration at the collagen output with the experimental output validated the computational model. As expected, calculated values of κ were not dependent on ΔP.

Statistics

Two-tailed Student *t* tests were used to calculate all *P* values. Statistically significant differences were reported if $P<0.05$.

Results

Microfluidic Device for Measuring Clot Permeability and Contractility

A microfluidic device was designed to allow pressure-driven transthrombus permeation with simultaneous imaging of clot contractile dynamics under flow. The device has a blood and buffer inlet port, collagen scaffold, and 3 ports for pressure readings (P1, P2, P3) up to 50 mm Hg (Figure 1A and Figure I in the online-only Data Supplement). The downstream buffer and upstream whole blood flows merge into a narrow channel to create resistance and control the lumen pressure at the collagen site corresponding to (P2+P1)/2. The pressure readings in these locations allowed the pressure drop across the collagen to be controlled, thus allowing computer simulation (Figure 1B) of Darcy flow through the complex geometry assuming constant permeability of the collagen (Figure 1C). Exposing a 250 μm long×60 μm wide surface area of collagen (± linked lipidated TF) to whole blood flow provided a localized thrombotic site comparable with a previous device without permeation.[14] The side view of collagen made it possible to image the permeation of dyes and the morphology of fibrin and platelet deposits as they contracted (Figure 1D–1E).

Stopping Flow Caused Platelet and Clot Retraction

During permeability testing of platelet deposits (no thrombin), the interruption of blood flow resulted in a drastic contractile response of the newly formed clot (Figure 2 and Video S1). This retraction unexpectedly enhanced permeability because of the reconfiguration of the supporting collagen and opening of flow paths along the sides of the collagen (Figure 3). To investigate the contraction triggered by flow cessation, platelet deposits were formed for 10 minutes with embedded 50 nm fluorescent beads as fiduciary markers (inlet wall shear rate of 1130 s^{-1}). A wall shear rate of 1160 s^{-1} was used to reproduce rates found in capillaries where the pressure drops between the vessel lumen and interstitial space are known.[20,21] This shear rate is also in the range of arterial flows. After 10 minutes of thrombus formation, the flow was switched without interruption to buffer for 4.5 minutes and then flow was completely stopped. Switching the flow from blood to buffer prevented the arrival of new platelets and release of fresh ADP or TXA_2.[22,23] Thrombus structure was mapped before and after stopping the flow

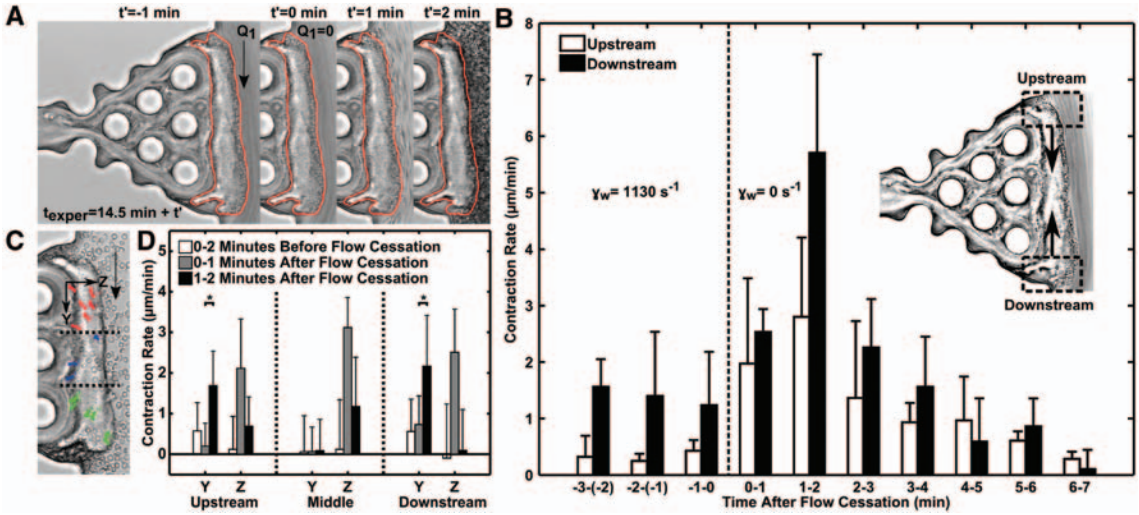

Figure 2. Flow arrest triggers clot contraction. A thrombus formed in the absence of thrombin and presence of fluorescent 50 nm beads was rinsed with Ca^{2+} buffer for 4.5 minutes before the cessation of flow caused a rapid contraction. The outline of a preretracted thrombus (t'=−1 minute) shows the inward retraction of the thrombus after flow stoppage (t'=0 to 2 minutes) (**A**). Contraction rate of the upstream and downstream sections of the thrombus were measured before and after flow arrest (n=3 donors) (**B**). Trajectories of the 50 nm beads represent the contractile response of the thrombus at upstream (red, n=6), middle (blue, n=3), and downstream (green, n=6) locations (**C**). Stopping the flow caused a significant increase in contraction rate in the Y and Z directions. To quantify these rates, the times before (0–2 minutes) and after flow cessation (0–1 minutes, 1–2 minutes) were monitored for bead velocity in the 3 sections of the thrombus (**D**). Downstream contraction rate in Y direction is shown as absolute value for contraction toward the middle region. **P*<0.01; error bars indicate mean±SD.

(Figure 2A). The upstream and downstream edge contraction rates were measured throughout the buffer flow period and after flow stoppage (Figure 2B). Contraction rates 1 to 2 minutes after flow cessation significantly increased by 6.5-fold (upstream region) and 4.6-fold (downstream region; $P<0.05$), compared with the rate during buffer flow. Donor-to-donor variability (n=3 donors) for total clot contraction, 7 minutes after flow arrest, was 8.93±3.89 μm and 13.6±4.42 μm at the upstream and downstream positions, respectively. The restructuring of the thrombus upstream and downstream edges by 2 minutes postflow cessation resulted in contractile trajectories of embedded beads toward the center of the thrombus mass (Figure 2C and Figure IIC in the online-only Data Supplement). Comparisons of the time-dependent contraction data in the Y and Z directions at upstream and downstream positions of the clot demonstrated increased contraction rates after flow cessation (Figure 2D). Movement in the +Z direction occurred rapidly and simultaneously in the upstream, downstream, and middle positions because of an immediate rebound effect caused by a reduced pressure drop and reduced permeation when the flow was stopped (Figure II in the online-only Data Supplement). Total bead distance in the Y and Z directions shows the rates at which the clot contracts in all 3 locations (Figure II in the online-only Data Supplement). The ≈1-minute delay in contraction in the Y direction is 1 indicator of an active signaling mechanism that must be engaged after the cessation in flow.

Permeability of Collagen, Platelet Deposits, and Platelet-Fibrin Thrombus Without Flow Interruption

To measure permeability without triggered thrombus contraction, dye tracer was pulsed immediately after whole blood flow without interruption of the flow. Inlet and outlet concentrations were measured with time to determine the permeation velocity at several physiologic pressure drops.[20,21] Permeability was numerically calculated over the complex geometry (Figure 3A–B) by reducing the squared error between the experimental and simulation permeation velocity. We validated this approach by comparing our calculated collagen permeability ($\kappa_{collagen}=1.98\times10^{-11}\pm0.640\times10^{-11}$ cm^2) with previous literature values (Figure 3C).[18,19] Similarly, permeation velocity was measured across platelet deposits and platelet-fibrin thrombi formed on collagen or TF/collagen scaffolds, respectively. Simulations that accurately predicted the experimentally measured output of dye concentration during the course of these experiments allowed determination of the permeability of the thrombus (Figure 3A–B). The resulting permeabilities for platelet deposits ($\kappa_{platelet}=5.45\times10^{-14}\pm0.898\times10^{-14}$ cm^2) and platelet-fibrin thrombus ($\kappa_{thrombus}=2.71\times10^{-14}\pm0.377\times10^{-14}$ cm^2) formed after 10 minutes of flow quantify the resistance that each structure provides to resist bleeding. In the absence of thrombin, PPACK-treated whole blood formed a platelet mass that was >350-fold less permeable than collagen alone. The presence of thrombin and formation of fibrin provided a further 50% reduction in permeability under hemodynamic conditions. Comparing the measured platelet deposit permeability (without flow interruption) with that obtained after flow interruption ($\kappa_{interrupted}=2.91\times10^{-13}\pm0.745\times10^{-13}$ cm^2) demonstrated the impact that stopping the flow had on the ability of the platelet deposit to maintain hemostasis in our device. In addition to permeability measurements, we observed decreased platelet accumulation with increased pressure drop (13.8 versus 23.4 mm Hg) across the intraluminal thrombus in PPACK-treated whole blood

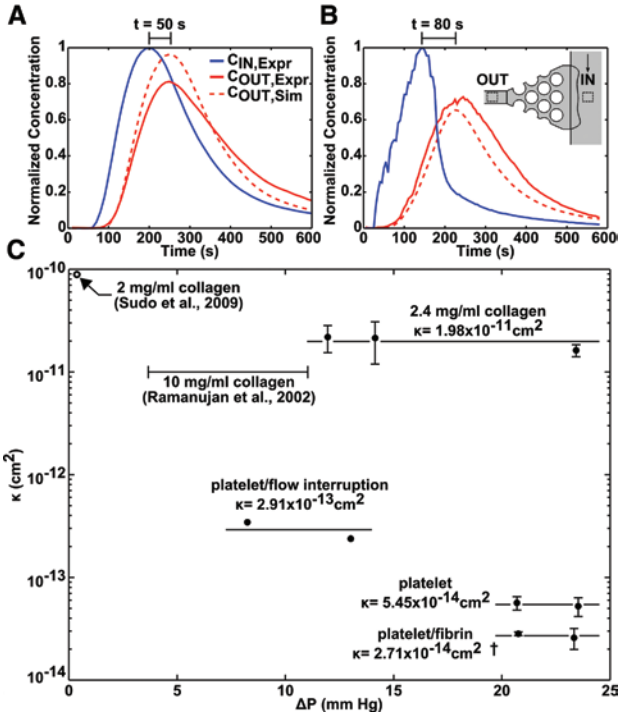

Figure 3. Clot permeability. Thrombi formed under 1130 s^{-1} were pulsed with fluorescent dye at controlled pressure drops. The normalized input and output fluorescent intensities, along with a numerically predicted output from COMSOL were measured over time for clots formed in the absence (**A**) and presence of tissue factor (TF) (**B**). Thrombus formed without thrombin reduced the residence time of the permeated dye by 30 seconds compared with platelet/fibrin thrombus. COMSOL simulations were used to numerically calculate permeability over collagen (n=9), platelet (n=6, 5 donors), platelet/fibrin (n=4, 4 donors), and platelet/low interrupted (n=2, 2 donors) geometries at constant pressure drops (**C**). †, $P<0.01$; error bars indicate mean±SD.

(Figure III in the online-only Data Supplement), likely because of increased transthrombus permeation of ADP and TXA_2 into the collagen.

Clot Retraction in a Rigid Wall Flow Device With Flow Reduction or Cessation

Clot retraction was also examined in a rigid, impermeable parallel-plate microfluidic device lacking transthrombus permeation. Clot development in PPACK-treated whole blood was imaged on a 250 µm×250 µm area of glass-supported fibrillar collagen at an initial wall shear rate of 1160 s^{-1}. Flow cessation resulted in an ≈10 µm contraction (upstream region) toward the center of the thrombus as outlined in Figure 4A. In comparison, by switching to 10 µmol/L blebbistatin perfusion (without flow disruption) for 7 minutes before the flow cessation, clot retraction after flow cessation was reduced 90% to only ≈1 µm (Figure 4B). Blebbistatin is a well-established platelet myosin IIA ATPase inhibitor.[24] In a scenario where flow was reduced from arterial (2000 s^{-1}) to venous (100 s^{-1}) shear rates, total contraction was similar to that observed with flow cessation. Also, the contraction was ≈5 µm larger than stopping the flow after blebbistatin treatment (Figure IV in the online-only Data Supplement). This result demonstrates the

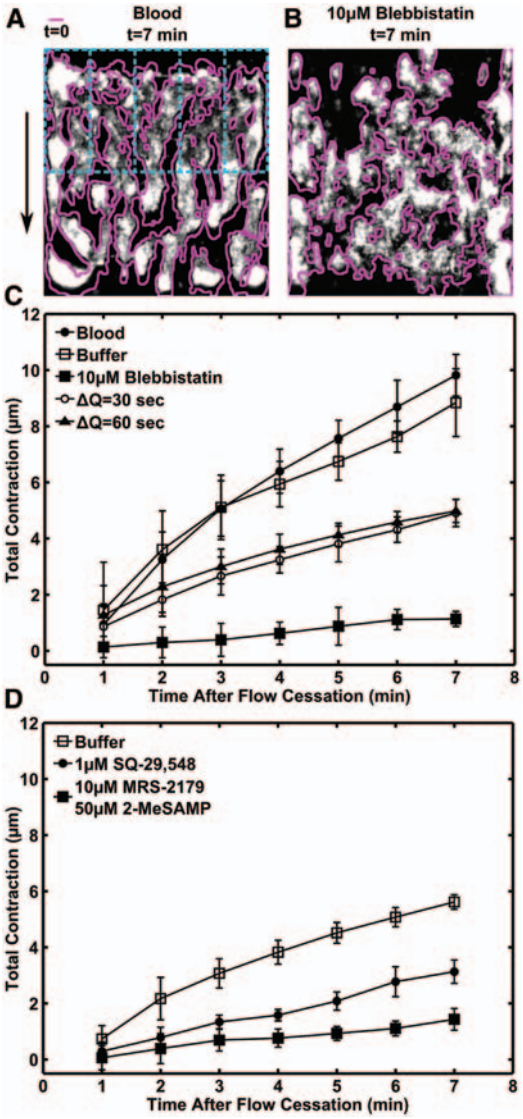

Figure 4. Contraction after flow arrest requires myosin and released ADP/thromboxane A2 (TXA_2). A parallel channel microfluidic device was used to develop thrombus in PPACK, at 1160 s^{-1}. After the formation of stable thrombi, Ca^{2+} or antagonist buffer was used to rinse the surface for 7 minutes before stopping flow. Upstream contractions were observed in 5 sections (blue dashed line) over 10 minutes. Stopping flow without a buffer rinse (**A**) and with a 10 µmol/L blebbistatin rinse (**B**) show clot retraction compared with a trace (pink line) before flow cessation. Total clot contraction measured over time compares the effects of blebbistatin and intermediate flow stopping with stopping flow with and without a buffer rinse (**C**). TXA_2 and ADP antagonist significantly reduced total contraction after flow cessation as compared with buffer (**D**). n=3 events at 5 discrete points for each time-point indicated, using 5 separate donors; error bars indicate mean±SD.

requirement of platelet myosin IIA activity in the triggered thrombus contraction after flow reduction or cessation.

We also measured clot retraction while stopping and restarting flow after a 30 seconds or 1 minute interruption (Figure 4C). Statistical differences between complete cessation of blood or buffer and the 30-seconds flow interruption became apparent after 1 minute. Interrupting flow for 1

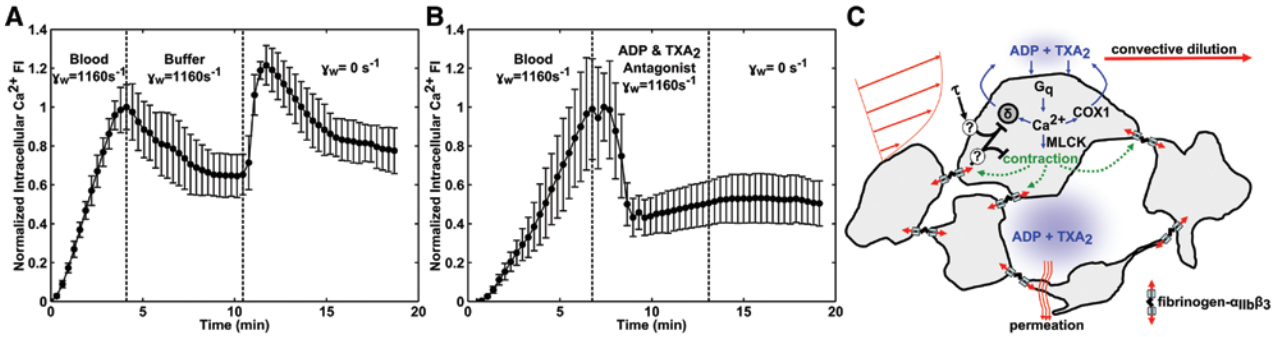

Figure 5. Flow cessation triggers platelet intracellular calcium mobilization via ADP/thromboxane A2 (TXA_2) autocrine signaling. Platelets in PPACK whole blood were loaded with Ca^{2+} dye and perfused over collagen at 1160 s^{-1}. After thrombus formation, whole blood perfusion was switched to Ca^{2+} or antagonist buffer for 6 minutes before stopping flow. Intracellular Ca^{2+} was measured via fluorescent intensity over time for either a Ca^{2+} buffer (**A**) or ADP and TXA_2 antagonist rinse (**B**). n=3 events using 2 donors, error bars indicate mean±SD. A schematic illustrates the flow sensing ability of platelets via convective removal of ADP/TXA_2 (**C**). Shear (τ) acting on the exterior of aggregated platelets accompanied by the strain placed on interconnected $\alpha_{IIb}\beta_3$ may signal the inhibition of contraction or dense granule (δ) release.

minute took 2 minutes to diverge statistically from complete flow cessation in buffer. Although neither of the temporary flow interruptions (30 seconds or 1 minute) were statistically different from each other, the longer 1-minute delay provided sufficient time to engage the contraction mechanism before eventually being diminished by the return of flow. The technique of switching to a nonphysiologic buffer and measuring contraction was validated by showing no contractile differences between stopping the flow in blood or stopping buffer flow after 7 minutes of rinsing.

Because flow cessation results in a dramatic change in both wall shear stress and wall shear rate on the thrombus structure, we investigated the role of soluble autocrine mediators whose concentration may change when flow is stopped. To explore the role of TXA_2, we added 1 μmol/L SQ-29,548, a potent TXA_2 receptor antagonist.[25] Additionally, the contribution of ADP was investigated by adding 10 μmol/L MRS-2179 and 50 μmol/L 2-MeSAMP, selective inhibitors of the $P2Y_1$ and $P2Y_{12}$ platelet receptors, respectively.[26] The dose–response curves for these inhibitors have been well established, and the final concentrations used under flow exceeded the experimentally determined the half maximal inhibitory concentration values to ensure complete inhibition.[25,26] After 7 minutes of buffer/antagonist perfusion, flow was stopped and total contraction was measured with time (Figure 4D). Both antagonists significantly reduced the total clot contraction as compared with buffer. ADP antagonists had the largest effect, reducing the total contraction nearly 75% during 7 minutes, whereas TXA_2 antagonist reduced the contraction by 44%. Although uninhibited contraction can vary significantly between donors (≈32%–44%), the addition of antagonist results in consistent donor-to-donor percent reductions that vary <7% for ADP and <3% for TXA_2. These findings demonstrate that ADP (from dense granules) and TXA_2 from activated cyclooxygenase-1 were the mediators of the triggered contraction response on flow cessation.

Intracellular Calcium Mobilization Is Triggered by ADP and TXA_2 After Flow Cessation

To explore the role of ADP and TXA_2 in the flow sensing by the thrombus, we loaded platelets in PPACK-treated whole blood with Ca^{2+} sensitive dye fluo-4. Before flow cessation, we treated the platelet deposits with buffer in the presence and absence of a triple cocktail of 1 μmol/L SQ-29,548, 10 μmol/L MRS-2179, and 50 μmol/L 2-MeSAMP. To minimize the measured intracellular Ca^{2+} fluctuations before flow cessation, initial contraction measurements were made 3 minutes after treatment and 3 minutes before flow arrest. The calcium signal increased as the platelet mass accumulated on the collagen between 0 and 4 minutes. When flow was switched to buffer at 4 minutes, there was no further deposition of platelets resulting in a slight decrease in signal. In the absence of inhibitors, flow cessation at 10 minutes caused an immediate and substantial mobilization of intracellular calcium (Figure 5A) that was completely blocked by the triple inhibitor cocktail to antagonize ADP and TXA_2 (Figure 5B). The calcium mobilization occurred within seconds after flow cessation and preceded the maximum platelet contraction rate which began 1 to 2 minutes after flow stoppage (Figure V in the online-only Data Supplement).

The triggered contraction by the platelet mass, after flow cessation, is an active material response requiring myosin (Figure 4C) and represents a flow sensing mechanism to impede contraction when flow is present. ADP and TXA_2 are the soluble mediators responsible for this response (Figures 4D and Figure 5B). Both of these agonists are highly sensitive to convective dilution which controls their concentrations in the boundary layer around the thrombus.[27] Because soluble species mediated Ca^{2+} mobilization and contraction on flow cessation, the flow sensing involved a transport mechanism: flow dilutes soluble species and flow cessation allows a rapid accumulation of autocrinic ADP and TXA_2 to trigger G_q signaling via platelet $P2Y_1$, $P2Y_{12}$, and thromboxane receptor receptors (Figure 5C).

Discussion

We report a novel hemodynamic sensing function of intraluminal blood clots. Flow impedes clot retraction. When flow stops, intraluminal clots retract more rapidly and to a greater extent. This hemodynamic sensing by platelets

in thrombus involves a rapid mobilization of calcium that strictly requires released ADP and TXA_2. Myosin activity is also required for the triggered contraction on flow cessation, indicating that the contraction is not a passive material response to reduced drag forces. This concept of a triggered, active response is also consistent with the ≈1 minute delay between flow cessation and enhanced contraction.

Although platelet contraction of a clot is usually considered in an isotropic context where blood is clotted in a tube and then detached from the glass walls to allow contraction, intraluminal thrombus formation is fundamentally different. In an isotropic assay, platelets have random orientation within a fibrin network whereas platelets depositing under flow conditions spread on collagen and then form many more platelet–platelet interactions because of high platelet concentration in the thrombus. In the thrombus formed under flow, the structure is less isotropic and spread platelets would be expected to exert greater forces along their axis of spreading and lesser forces perpendicular to the plane of spreading. Furthermore, clotted whole blood in a tube contains incompressible red blood cells at the prevailing hematocrit, whereas thrombus formed under arterial flow are greatly enriched in platelets (50-100 × platelet rich plasma levels) and substantially depleted of red blood cells.

Despite recent advances in microfluidic devices and intravital mouse microscopy, few tools are available to control and study the effects of thrombus permeation under flow conditions. Recent studies examining angiogenesis demonstrated microfluidic devices that hold promise for studying in vitro clot permeability under flow conditions.[19,28] However, these designs lacked the potential to produce controllable pressure drops and shear rates relevant to thrombosis and hemostasis. In the present study, we designed a microfluidic device to develop whole blood clots under physiologic flow and to investigate transthrombus permeation in the presence of a controlled pressure drop. The microfluidic device allowed the first reported in vitro clot permeability for clots formed under flow. Although a measurement for the permeability of a contracted clot could not be obtained because of the accompanied structural changes in the absence of endothelium, it is expected to be less than that of a nonretracted platelet-fibrin deposit. Our measurement for these deposits represents a quantitatively important upper bound of the contracted clot permeability and the associated inner clot transport of ADP and TXA_2. Interestingly, the permeability of healthy rabbit aortic wall is on the order of 10^{-14} cm^2,[29] which is quite similar to our measurement of a platelet-fibrin thrombus. This suggests that a platelet-rich intraluminal thrombus has a permeability that is well matched to the surrounding intact endothelium. In addition to matching rigidity,[3] an intraluminal thrombus may match permeability to the surrounding vessel wall. Under flow conditions, we propose flow sensing helps the spread platelet(s) maintain hemostatic function by balancing the contractile apparatus with the applied flow to limit platelet contraction because contraction would potentially create gaps for leakage or alter nearby endothelial function.

In a quantitatively more intense example of hemostasis, a blunt impact that compresses a vessel without rupturing the vessel would be expected to cause more extensive endothelial denudation. This situation is perhaps most analogous to the experimental configuration developed in this study. When blood flow is maintained in such an injured vessel, the flow impedes clot contraction because wound closure would not be needed. Also occlusion might be prevented because clot stabilization via contraction is impeded by flow. Reduced ADP/TXA_2 transport may also facilitate the formation of a dense inner thrombus core,[30] whereas the outer domains of the clot remain loose and friable because of flow sensing. Throughout our studies with multiple donors, this was repeatedly verified by the constant but relatively low contraction rate under flow (Figure 2B and Figure VI in the online-only Data Supplement). As vessel injury becomes severe enough to cause vessel rupture with blood leaving the vascular space, blood pools around the puncture/rupture/severed site. This results in more isotropic clotting of whole blood, which can exert isotropic contraction on the surrounding tissue to facilitate wound closure and consequently hemostasis (Figure VII in the online-only Data Supplement). In this situation, the pooled blood around a leaking vessel is not subjected to substantial hemodynamic flow to dilute ADP/TXA_2 and thus impair platelet actinomyosin-mediated contraction. Additional highly diffusible platelet activators may also play a role in this observed contraction and provide an area of future study.

To further investigate the novel flow sensing abilities of platelets we examined their ability to contract after 30 seconds or 1-minute interruptions in flow. Contraction rates initially followed previous experiments but were drastically dampened on the return of flow (Figure VIII in the online-only Data Supplement). This result suggests that the quasi-steady state that platelet deposits reach under hemodynamic forces preserves their ability to rapidly contract in response to flow arrest. Flow sensing by a thrombus balances the need for wound closure and hemostasis against the risk of intraluminal occlusive thrombosis with dense contracted and lytic-resistant structures.[31] In cases of normal hemostasis, this mechanism would allow clots to contract gradually from their interior toward their exterior as hemodynamic flow is reduced. The extent to which stress present in the thrombus plays a role in signaling (ie, mechanotransduction) remains a subject of future study. These experiments clearly demonstrate the ability of platelet deposits to rapidly assemble into a hemodynamic sensor and contract on the arrest of flow.

Acknowledgment

We thank Thomas V. Colace for guidance in design and microfabrication of microfluidic devices.

Sources of Funding

This study was supported by National Institutes of Health, NIH R01 HL103419 (Dr Diamond).

Disclosures

None.

References

1. Laurens N, Koolwijk P, de Maat MP. Fibrin structure and wound healing. *J Thromb Haemost*. 2006;4:932–939.
2. Jen CJ, McIntire LV. The structural properties and contractile force of a clot. *Cell Motil*. 1982;2:445–455.
3. Lam WA, Chaudhuri O, Crow A, Webster KD, Li TD, Kita A, Huang J, Fletcher DA. Mechanics and contraction dynamics of single platelets and implications for clot stiffening. *Nat Mater*. 2011;10:61–66.
4. Adelstein RS. Calmodulin and the regulation of the actin-myosin interaction in smooth muscle and nonmuscle cells. *Cell*. 1982;30:349–350.
5. Suzuki Y, Yamamoto M, Wada H, Ito M, Nakano T, Sasaki Y, Narumiya S, Shiku H, Nishikawa M. Agonist-induced regulation of myosin phosphatase activity in human platelets through activation of Rho-kinase. *Blood*. 1999;93:3408–3417.
6. Haling JR, Monkley SJ, Critchley DR, Petrich BG. Talin-dependent integrin activation is required for fibrin clot retraction by platelets. *Blood*. 2011;117:1719–1722.
7. Leisner TM, Parise LV. Talin's second act-ivation: retraction. *Blood*. 2011;117:1442–1443.
8. Diamond SL. Engineering design of optimal strategies for blood clot dissolution. *Annu Rev Biomed Eng*. 1999;1:427–462.
9. Zidansek A, Blinc A, Lahajnar G, Keber D, Blinc R. Finger-like lysing patterns of blood clots. *Biophys J*. 1995;69:803–809.
10. Spero RC, Sircar RK, Schubert R, Taylor RM 2nd, Wolberg AS, Superfine R. Nanoparticle diffusion measures bulk clot permeability. *Biophys J*. 2011;101:943–950.
11. Kudryk B, Rohoza A, Ahadi M, Chin J, Wiebe ME. Specificity of a monoclonal antibody for the NH2-terminal region of fibrin. *Mol Immunol*. 1984;21:89–94.
12. Litvinov RI, Gorkun OV, Galanakis DK, Yakovlev S, Medved L, Shuman H, Weisel JW. Polymerization of fibrin: Direct observation and quantification of individual B:b knob-hole interactions. *Blood*. 2007;109:130–138.
13. Duffy DC, McDonald JC, Schueller OJ, Whitesides GM. Rapid Prototyping of Microfluidic Systems in Poly(dimethylsiloxane). *Anal Chem*. 1998;70:4974–4984.
14. Neeves KB, Maloney SF, Fong KP, Schmaier AA, Kahn ML, Brass LF, Diamond SL. Microfluidic focal thrombosis model for measuring murine platelet deposition and stability: PAR4 signaling enhances shear-resistance of platelet aggregates. *J Thromb Haemost*. 2008;6:2193–2201.
15. Colace TV, Muthard RW, Diamond SL. Thrombus growth and embolism on tissue factor-bearing collagen surfaces under flow: role of thrombin with and without fibrin. *Arterioscler Thromb Vasc Biol*. 2012;32:1466–1476.
16. Colace TV, Jobson J, Diamond SL. Relipidated tissue factor linked to collagen surfaces potentiates platelet adhesion and fibrin formation in a microfluidic model of vessel injury. *Bioconjug Chem*. 2011;22:2104–2109.
17. Smith SA, Morrissey JH. Rapid and efficient incorporation of tissue factor into liposomes. *J Thromb Haemost*. 2004;2:1155–1162.
18. Ramanujan S, Pluen A, McKee TD, Brown EB, Boucher Y, Jain RK. Diffusion and convection in collagen gels: implications for transport in the tumor interstitium. *Biophys J*. 2002;83:1650–1660.
19. Sudo R, Chung S, Zervantonakis IK, Vickerman V, Toshimitsu Y, Griffith LG, Kamm RD. Transport-mediated angiogenesis in 3D epithelial coculture. *FASEB J*. 2009;23:2155–2164.
20. Wiig H. Evaluation of methodologies for measurement of interstitial fluid pressure (Pi): physiological implications of recent Pi data. *Crit Rev Biomed Eng*. 1990;18:27–54.
21. Parazynski SE, Hargens AR, Tucker B, Aratow M, Styf J, Crenshaw A. Transcapillary fluid shifts in tissues of the head and neck during and after simulated microgravity. *J Appl Physiol*. 1991;71:2469–2475.
22. Beigi R, Kobatake E, Aizawa M, Dubyak GR. Detection of local ATP release from activated platelets using cell surface-attached firefly luciferase. *Am J Physiol*. 1999;276:C267–C278.
23. De Caterina R, Giannessi D, Gazzetti P, Bernini W. Thromboxane-B2 generation during ex-vivo platelet aggregation. *J Nucl Med Allied Sci*. 1984;28:185–196.
24. Johnson GJ, Leis LA, Krumwiede MD, White JG. The critical role of myosin IIA in platelet internal contraction. *J Thromb Haemost*. 2007;5:1516–1529.
25. Ogletree ML, Harris DN, Greenberg R, Haslanger MF, Nakane M. Pharmacological actions of SQ 29,548, a novel selective thromboxane antagonist. *J Pharmacol Exp Ther*. 1985;234:435–441.
26. Maloney SF, Brass LF, Diamond SL. P2Y12 or P2Y1 inhibitors reduce platelet deposition in a microfluidic model of thrombosis while apyrase lacks efficacy under flow conditions. *Integr Biol (Camb)*. 2010;2:183–192.
27. Flamm MH, Colace TV, Chatterjee MS, Jing H, Zhou S, Jaeger D, Brass LF, Sinno T, Diamond SL. Multiscale prediction of patient-specific platelet function under flow. *Blood*. 2012;120:190–198.
28. Vickerman V, Blundo J, Chung S, Kamm R. Design, fabrication and implementation of a novel multi-parameter control microfluidic platform for three-dimensional cell culture and real-time imaging. *Lab Chip*. 2008;8:1468–1477.
29. Tedgui A, Lever MJ. Filtration through damaged and undamaged rabbit thoracic aorta. *Am J Physiol*. 1984;247(5 pt 2):H784–H791.
30. Brass L. Understanding and evaluating platelet function. *Hematology Am Soc Hematol Educ Program*. 2010;2010:387–396.
31. Sabovic M, Lijnen HR, Keber D, Collen D. Effect of retraction on the lysis of human clots with fibrin specific and non-fibrin specific plasminogen activators. *Thromb Haemost*. 1989;62:1083–1087.